Rapid Communications

Search for the rare decay $\Lambda_c^+ \to p\mu^+\mu^-$

R. Aaij *et al.*[*]
(LHCb Collaboration)

(Received 21 December 2017; published 4 May 2018)

A search for the flavor-changing neutral-current decay $\Lambda_c^+ \to p\mu^+\mu^-$ is reported using a data set corresponding to an integrated luminosity of 3.0 fb^{-1} collected by the LHCb Collaboration. No significant signal is observed outside of the dimuon mass regions around the ϕ and ω resonances, and an upper limit is placed on the branching fraction of $\mathcal{B}(\Lambda_c^+ \to p\mu^+\mu^-) < 7.7(9.6) \times 10^{-8}$ at 90%(95%) confidence level. A significant signal is observed in the ω dimuon mass region for the first time.

DOI: 10.1103/PhysRevD.97.091101

The flavor-changing neutral-current (FCNC) decay $\Lambda_c^+ \to p\mu^+\mu^-$ (inclusion of the charge-conjugate processes is implied throughout) is expected to be heavily suppressed in the Standard Model (SM) by the Glashow-Iliopoulos-Maiani mechanism [1]. The branching fractions for short-distance $c \to u\ell^+\ell^-$ contributions to the transition are expected to be of $\mathcal{O}(10^{-9})$ in the SM but can be enhanced by effects beyond the SM. However, long-distance contributions proceeding via a tree-level amplitude, with an intermediate meson resonance decaying into a dimuon pair [2,3], can increase the branching fraction up to $\mathcal{O}(10^{-6})$ [4]. The short-distance and hadronic contributions can be separated by splitting the data set into relevant regions of dimuon mass. The $\Lambda_c^+ \to p\mu^+\mu^-$ decay has been previously searched for by the *BABAR* Collaboration [5], yielding $11.1 \pm 5.0 \pm 2.5$ events and an upper limit on the branching fraction of 4.4×10^{-5} at 90% C.L.

Similar FCNC transitions for the b-quark system ($b \to s\ell^+\ell^-$) exhibit a pattern of consistent deviations from the current SM predictions both in branching fractions [6] and angular observables [7], with the combined significance reaching 4 to 5 standard deviations [8,9]. Processes involving $c \to u\ell^+\ell^-$ transitions are far less explored at both the experimental and theoretical levels, which makes such measurements desirable. Similar analyses of the D system have reported evidence for the long-distance contribution [10]; however, the short-distance contributions have not been established [11].

In this paper, we report on the search for the $\Lambda_c^+ \to p\mu^+\mu^-$ decay, using a data set corresponding to an integrated luminosity of 3.0 fb^{-1} of pp collisions collected in 2011 and 2012 with the LHCb experiment. The branching fraction is measured with respect to the branching fraction of the decay $\Lambda_c^+ \to p\phi(1020)$ with $\phi(1020) \to \mu^+\mu^-$ [here and after denoted as $\Lambda_c^+ \to p\phi(\mu^+\mu^-)$] decay, which has the benefit of having the same initial and final states, and consequently many sources of systematic uncertainty are expected to cancel.

The LHCb detector [12,13] is a single-arm forward spectrometer covering the pseudorapidity range $2 < \eta < 5$, designed for the study of particles containing b or c quarks. The detector includes a high-precision tracking system consisting of a silicon-strip vertex detector surrounding the pp interaction region [14], a large-area silicon-strip detector located upstream of a dipole magnet with a bending power of about 4 Tm, and three stations of silicon-strip detectors and straw drift tubes [15] placed downstream of the magnet. The tracking system provides a measurement of momentum, of charged particles with a relative uncertainty that varies from 0.5% at low momentum to 1.0% at 200 GeV/c. The minimum distance of a track to a primary vertex (PV), the impact parameter, is measured with a resolution of $(15 + 29/p_{\mathrm{T}})$ μm, where p_{T} is the component of the momentum transverse to the beam, in GeV/c. Different types of charged hadrons are distinguished using information from two ring-imaging Cherenkov detectors [16]. Photons, electrons, and hadrons are identified by a calorimeter system consisting of scintillating-pad and preshower detectors, an electromagnetic calorimeter, and a hadronic calorimeter. Muons are identified by a system composed of alternating layers of iron and multiwire proportional chambers [17]. The online event selection is performed by a trigger [18], which consists of a hardware stage, based on information from the calorimeter and muon systems, followed by a software stage, which applies a full event reconstruction.

Samples of simulated events are used to understand the properties of the signal and normalization channels. The pp collisions are generated using PYTHIA [19] with a specific LHCb configuration [20]. Decays of hadronic particles are

[*]Full author list given at end of the article.

described by EvtGen [21], in which final-state radiation is generated using Photos [22]. The decay of the Λ_c^+ baryon to $p\,\mu^+\mu^-$ is simulated with a three-body phase-space model. The interaction of the generated particles with the detector and its response are implemented using the Geant4 toolkit [23] as described in Ref. [24]. The Λ_c^+ baryons are produced in two ways at a hadron collider: as prompt Λ_c^+ or in b-hadron decays. The simulation contains a mixture of these two production mechanisms, according to the known Λ_c^+ and b-hadron production cross sections [25,26].

The simulated samples are used to determine the selection criteria, in particular to train a multivariate classifier that is aimed at distinguishing signal signatures in the background-dominated data set. The simulated samples are also used to calculate the efficiencies of several selection steps.

Candidate events of $\Lambda_c^+ \to p\mu^+\mu^-$ decay are reconstructed by combining a pair of charged tracks identified as muons with one identified as a proton. Candidates that pass the trigger selections are subject to further requirements consisting of kinematic and particle-identification criteria and based on the response of a multivariate classifier. Each of the final-state tracks is required to be of good quality, to have $p_T > 300$ MeV/c, and to be incompatible with originating from any of the PVs in the event. The tracks are also required to form a good-quality secondary vertex with a corresponding flight distance of at least 0.1 mm from all of the PVs in the event. The invariant mass of the dimuon system is required to be smaller than 1400 MeV/c^2. Three dimuon mass regions are defined:

(i) A region around the known ϕ mass, [985, 1055] MeV/c^2, used as a normalization channel.
(ii) A region around the known ω mass [the ω denotes hereafter the $\omega(782)$ meson], [759, 805] MeV/c^2, used to isolate the $\Lambda_c^+ \to p\omega$ decay.
(iii) A nonresonant region ($\Lambda_c^+ \to p\mu^+\mu^-$), with excluded ranges ± 40 MeV/c^2 around the known ω and ϕ masses.

After the preselection, the normalization channel is still dominated by the combinatorial background, i.e. combinations of tracks that do not all originate from a genuine Λ_c^+ baryon. A boosted decision tree (BDT) is trained to reduce the combinatorial background to a manageable level. The BDT is trained using the kinematic and topological variables of the Λ_c^+ candidate, related to its flight distance, decay vertex quality, p_T, and impact parameter with respect to the primary vertex. In the BDT training, $\Lambda_c^+ \to p\mu^+\mu^-$ simulated events are used as a proxy for the signal, and data outside the signal $p\,\mu^+\mu^-$ invariant-mass region extending up to ± 300 MeV/c^2 around the known Λ_c^+ mass are used as a proxy for the background.

A k-folding technique is used to ensure the training is unbiased [27], while keeping the full available data sets for further analysis. A loose BDT cut is applied to reduce the background to the same level as the normalization channel yield.

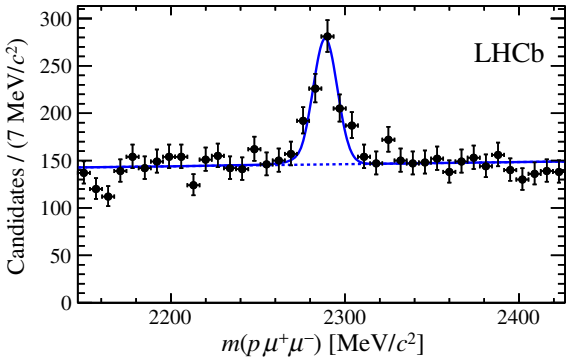

FIG. 1. Mass distribution of $\Lambda_c^+ \to p\mu^+\mu^-$ candidates in the ϕ region after the first BDT requirement. The solid line shows the result of the fit described in the text, while the dashed line indicates the background component.

A fit to the $p\mu^+\mu^-$ invariant-mass distribution of $\Lambda_c^+ \to p\phi(\mu^+\mu^-)$ candidates after the loose BDT requirement is shown in Fig. 1. The shape of the Λ_c^+ peak is parametrized by a Crystal Ball function [28] with parameters determined from the simulation, while the background is modeled with a first-order polynomial. The yield of the $\Lambda_c^+ \to p\phi(\mu^+\mu^-)$ decay is determined to be 395 ± 45 candidates. This sample is used for the final optimization of selection requirements. It is checked at this stage that the variables used in the signal selection are well described by simulation within the available sample size.

For the final selection, a second BDT, which includes additional variables related to Λ_c^+ -baryon decay properties and the isolation of the proton and muons in the detector, is trained. The final discrimination is performed in three dimensions: the BDT variable and two particle-identification (PID) variables, the proton-identification discriminant, and the muon-identification discriminant. The optimal set of BDT and PID requirements is determined by finding the best expected upper limit on the branching fraction of the signal relative to the normalization channel using the CL_s method [29] by means of Monte Carlo methods.

Several sources of background have been considered. An irreducible background due to long-distance contributions originates from $\Lambda_c^+ \to pV(\mu^+\mu^-)$ decays, with intermediate resonances indicated by V. The $\rho(770)^0$, ω, and η resonances are studied; however, their contribution to the nonresonant region is expected to be negligible, because the V meson mass is well separated from the nonresonant region and/or the $\Lambda_c^+ \to pV(\mu^+\mu^-)$ branching fraction is small. Another background source considered is due to misidentification of final-state particles in hadronic D^+, D_s^+, and Λ_c^+ decays. The expected contribution from this source has been estimated using large samples of simulated events. Given the tight PID requirements obtained from the optimization, only 2.0 ± 1.1 candidates are expected to fall into the Λ_c^+ mass window in the nonresonant region.

The ratio of branching fractions is measured using

$$\frac{\mathcal{B}(\Lambda_c^+ \to p\mu^+\mu^-)}{\mathcal{B}(\Lambda_c^+ \to p\phi)\mathcal{B}(\phi \to \mu^+\mu^-)} = \frac{\epsilon_{\rm norm}}{\epsilon_{\rm sig}} \times \frac{N_{\rm sig}}{N_{\rm norm}}, \quad (1)$$

where $N_{\rm sig}$ ($N_{\rm norm}$) is the observed yield for the signal (normalization) decay mode. The factors $\epsilon_{\rm sig}$ and $\epsilon_{\rm norm}$ indicate the corresponding total efficiencies for signal and normalization channels, respectively. The efficiencies are determined from the simulation.

In the case of the observation of the decay $\Lambda_c^+ \to pV$, the ratio of branching fractions is determined by

$$\frac{\mathcal{B}(\Lambda_c^+ \to pV)\mathcal{B}(V \to \mu^+\mu^-)}{\mathcal{B}(\Lambda_c^+ \to p\phi)\mathcal{B}(\phi \to \mu^+\mu^-)} = \frac{\epsilon_{\rm norm}}{\epsilon_V} \times \frac{N_V}{N_{\rm norm}}, \quad (2)$$

where N_V ($N_{\rm norm}$) is the number of candidates observed for the $\Lambda_c^+ \to pV$ (normalization) decay mode. The factors ϵ_V and $\epsilon_{\rm norm}$ indicate the corresponding total efficiencies for $\Lambda_c^+ \to pV$ and the normalization channel, respectively.

As the final states of the signal and normalization channels are identical, many sources of systematic uncertainty cancel in the ratio of the efficiencies. There are three significant sources of systematic uncertainty. The first is related to the finite size of the simulation samples, which limits the precision on the efficiency ratio. The second is linked to residual differences between data and simulation of the BDT distribution. The third is associated to the simulation of PID and is determined from the uncertainty on the PID calibration samples. The values of the contributions are given in Table I.

Several other sources of systematic uncertainty were considered: the trigger efficiency, the shapes used in the invariant-mass fit for signal and normalization channels, the shape of the combinatorial background, and the fraction of prompt Λ_c^+ baryons and Λ_c^+ baryons from b-hadron decays. All of these, however, are at negligible level when compared to three dominant sources of systematic uncertainty.

The simulated $\Lambda_c^+ \to p\mu^+\mu^-$ decays have been generated according to a phase-space model for the decay products. As the exact physics model for the decay is not known, no systematic uncertainty is assigned. Instead, the weights needed to recast the result in terms of any physics model are provided in Fig. 2. The weights are described by a function of the dimuon invariant-mass squared $m^2(\mu^+\mu^-)$ and the invariant mass of the proton and the negatively charged muon squared $m^2(p\mu^-)$. The weights are normalized to the average efficiency.

TABLE I. Systematic uncertainties on the efficiency ratio used in the determination of the branching fraction in the nonresonant and ω regions.

Uncertainty source	Value (%) $\Lambda_c^+ \to p\mu^+\mu^-$ nonresonant	Value (%0 $\Lambda_c^+ \to pV(\mu^+\mu^-)$ ω region
Size of simulation samples	4.4	10.0
BDT cut	4.8	4.8
PID cut	0.7	0.7
Total	6.5	11.1

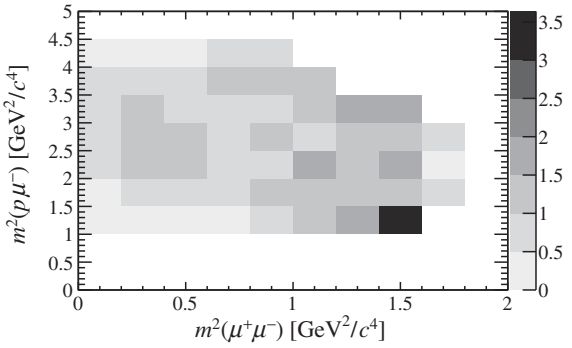

FIG. 2. The efficiency weights for $\Lambda_c^+ \to p\mu^+\mu^-$ as a function of the dimuon invariant mass squared $m^2(\mu^+\mu^-)$ and by the invariant mass of the proton and the negatively charged muon squared $m^2(p\mu^-)$. The weights are normalized to the average efficiency.

The distributions of the $p\ \mu^+\mu^-$ invariant mass for the $\Lambda_c^+ \to p\mu^+\mu^-$ candidates after final selections in the three dimuon mass ranges are presented in Fig. 3. The Λ_c^+ peak is parametrized by a Crystal Ball [28] function with parameters determined from the simulation, and the background is described by a first-order polynomial. The fits are used to determine the signal yields. No significant signal is observed in the nonresonant region [Fig. 3(a)]. The yield for the normalization channel is determined to be 96 ± 11 candidates [Fig. 3(b)]. An accumulation of 13.2 ± 4.3 candidates at the Λ_c^+ mass is observed in the ω region [Fig. 3(c)]. The statistical significance of the excess is determined to be 5.0σ using Wilks's theorem [30].

The distribution of the dimuon invariant mass of the Λ_c^+ candidates is shown in Fig. 4. An excess is seen at the known ω and ϕ resonance masses. The data are well described by a simple model including these resonances and a background component. The ω and ϕ peaks are parametrized as Breit-Wigner functions of relevant decay width [31] convolved with a Gaussian function to take into account the experimental resolution. The addition of a component for the $\rho(770)^0$ resonance (and its interference with the ω meson) does not improve the fit quality. It is therefore assumed that the observed candidates in the ω region are dominated by decays via the ω resonance.

As no evidence for nonresonant $\Lambda_c^+ \to p\mu^+\mu^-$ decays is found, an upper limit on the branching fractions is determined using the $\rm CL_s$ method. The systematic uncertainties are included in the construction of $\rm CL_s$. The following upper limits are obtained at different C.L.s:

$$\frac{\mathcal{B}(\Lambda_c^+ \to p\mu^+\mu^-)}{\mathcal{B}(\Lambda_c^+ \to p\phi)\mathcal{B}(\phi \to \mu^+\mu^-)} < 0.24(0.28) \quad \text{at } 90\%(95\%) \text{ C.L.}$$

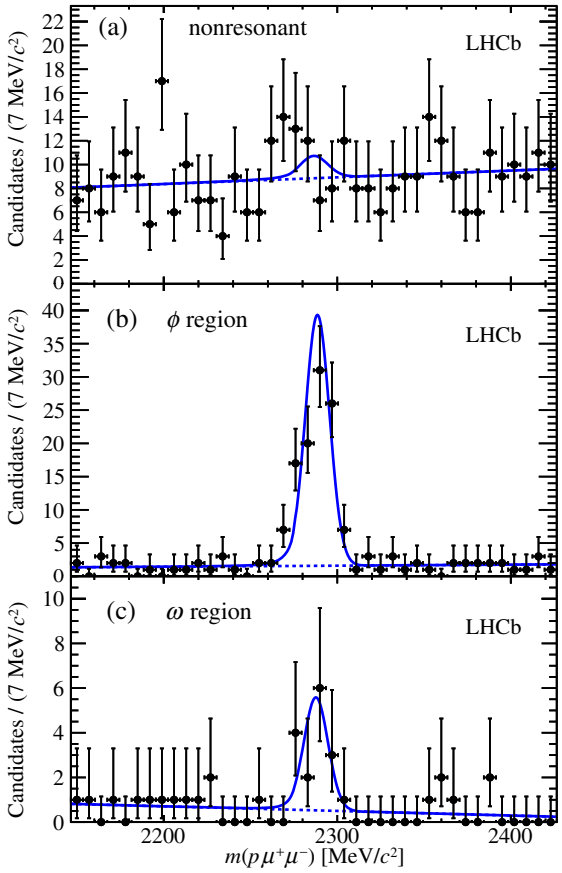

FIG. 3. Mass distribution for selected $p\,\mu^+\mu^-$ candidates in the three regions of the dimuon invariant mass: a) nonresonant region, b) ϕ region, and c) ω region. The solid lines show the results of the fit as described in the text. The dashed lines indicate the background component.

The corresponding distribution of CL_s is shown in Fig. 5. Using the values of the branching fractions for $\Lambda_c^+ \to p\phi$ and $\phi \to \mu^+\mu^-$ decays from Ref. [31] and including their uncertainties in the CL_s construction, an upper limit on the branching fraction is determined to be

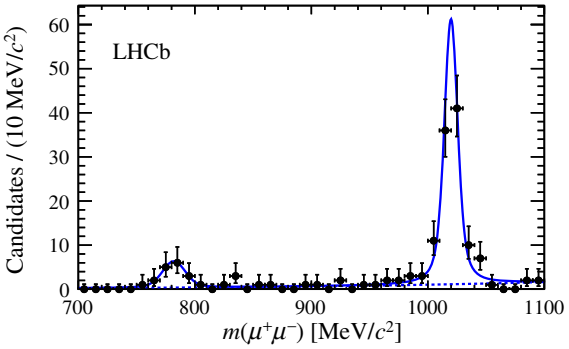

FIG. 4. Invariant-mass distribution $m(\mu^+\mu^-)$ for $\Lambda_c^+ \to p\mu^+\mu^-$ candidates with mass ± 25 MeV/c^2 around the Λ_c^+ mass. The solid line shows the result of the fit, while the dashed line indicates the background component.

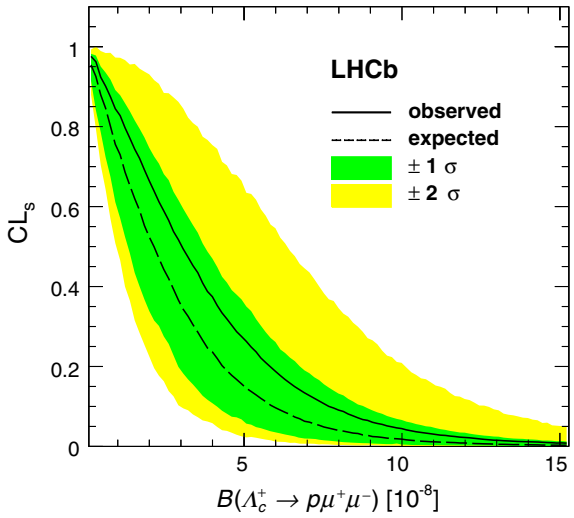

FIG. 5. The CL_s value as a function of the $\mathcal{B}(\Lambda_c^+ \to p\mu^+\mu^-)$ branching fraction. The median expected value of an ensemble (assuming no signal component) is shown by the dashed line, with the $\pm 1\sigma$ and $\pm 2\sigma$ regions shaded. The observed distribution is shown by the solid line.

$$\mathcal{B}(\Lambda_c^+ \to p\mu^+\mu^-) < 7.7(9.6) \times 10^{-8} \quad \text{at } 90\%(95\%) \text{ C.L.}$$

Under the above-mentioned assumption of the $\Lambda_c^+ \to p\omega$ dominance in the ω region, the relative branching fraction with respect to the normalization channel is determined according to Eq. (2):

$$\frac{\mathcal{B}(\Lambda_c^+ \to p\omega)\mathcal{B}(\omega \to \mu^+\mu^-)}{\mathcal{B}(\Lambda_c^+ \to p\phi)\mathcal{B}(\phi \to \mu^+\mu^-)} = 0.23 \pm 0.08\ (\text{stat}) \pm 0.03\ (\text{syst}).$$

Using the relevant branching fractions from Ref. [31], the branching fraction of $\Lambda_c^+ \to p\omega$ is determined to be

$$\mathcal{B}(\Lambda_c^+ \to p\omega) = (9.4 \pm 3.2(\text{stat}) \pm 1.0(\text{syst}) \pm 2.0(\text{ext})) \times 10^{-4},$$

where the first uncertainty is statistical, the second corresponds to the above-mentioned systematic effects, and the third is due to the limited knowledge of the relevant branching fractions. Assuming lepton universality, the branching fraction $\mathcal{B}(\omega \to e^+e^-)$ is used instead of $\mathcal{B}(\omega \to \mu^+\mu^-)$.

In summary, a search for the $\Lambda_c^+ \to p\mu^+\mu^-$ decay is reported, using pp data collected with the LHCb experiment. The analysis is performed in three regions of dimuon mass: ϕ, ω, and nonresonant. The upper limit on the nonresonant mode is improved by 2 orders of magnitude with respect to the previous measurement [5]. For the first time, the signal is seen in the ω region with a statistical significance of five standard deviations.

ACKNOWLEDGMENTS

We express our gratitude to our colleagues in the CERN accelerator departments for the excellent performance of the LHC. We thank the technical and administrative staff at the LHCb institutes. We acknowledge support from CERN and from the national agencies CAPES, CNPq, FAPERJ, and FINEP (Brazil); MOST and NSFC (China); CNRS/IN2P3 (France); BMBF, DFG, and MPG (Germany); INFN (Italy); NWO (The Netherlands); MNiSW and NCN (Poland); MEN/IFA (Romania); MinES and FASO (Russia); MinECo (Spain); SNSF and SER (Switzerland); NASU (Ukraine); STFC (United Kingdom); and NSF (USA). We acknowledge the computing resources that are provided by CERN, IN2P3 (France), KIT and DESY (Germany), INFN (Italy), SURF (The Netherlands), PIC (Spain), GridPP (United Kingdom), RRCKI and Yandex LLC (Russia), CSCS (Switzerland), IFIN-HH (Romania), CBPF (Brazil), PL-GRID (Poland), and OSC (USA). We are indebted to the communities behind the multiple open-source software packages on which we depend. Individual groups or members have received support from AvH Foundation (Germany); EPLANET, Marie Skłodowska-Curie Actions and ERC (European Union); ANR, Labex P2IO and OCEVU, and Région Auvergne-Rhône-Alpes (France); RFBR, RSF and Yandex LLC (Russia); GVA, XuntaGal and GENCAT (Spain); and Herchel Smith Fund, the Royal Society, the English-Speaking Union and the Leverhulme Trust (United Kingdom).

[1] S. Glashow, J. Iliopoulos, and L. Maiani, Weak interactions with lepton-hadron symmetry, Phys. Rev. D **2**, 1285 (1970).
[2] S. Fajfer, A. Prapotnik, S. Prelovšek, P. Singer, and J. Zupan, The rare decays of D mesons, Nucl. Phys. B, Proc. Suppl. **115**, 93 (2003).
[3] G. Burdman, E. Golowich, J. L. Hewett, and S. Pakvasa, Rare charm decays in the standard model and beyond, Phys. Rev. D **66**, 014009 (2002).
[4] S. Fajfer and S. Prelovsek, Effects of littlest Higgs model in rare D meson decays, Phys. Rev. D **73**, 054026 (2006).
[5] J. P. Lees *et al.* (*BABAR* Collaboration), Searches for rare or forbidden semileptonic charm decays, Phys. Rev. D **84**, 072006 (2011).
[6] R. Aaij *et al.* (LHCb Collaboration), Measurement of the S-wave fraction in $B^0 \to K^+\pi^-\mu^+\mu^-$ decays and the $B^0 \to K^*(892)^0\mu^+\mu^-$ differential branching fraction, J. High Energy Phys. 11 (2016) 047; Erratum, J. High Energy Phys. 04 (2017) 142.
[7] R. Aaij *et al.* (LHCb Collaboration), Angular analysis of the $B^0 \to K^{*0}\mu^+\mu^-$ decay using 3 fb^{-1} of integrated luminosity, J. High Energy Phys. 02 (2016) 104.
[8] B. Capdevila, A. Crivellin, S. Descotes-Genon, J. Matias, and J. Virto, Patterns of New Physics in $b \to s\ell^+\ell^-$ transitions in the light of recent data, J. High Energy Phys. 01 (2018) 093.
[9] W. Altmannshofer, C. Niehoff, P. Stangl, and D. M. Straub, Status of the $B \to K^*\mu^+\mu^-$ anomaly after Moriond 2017, Eur. Phys. J. C **77**, 377 (2017).
[10] R. Aaij *et al.* (LHCb Collaboration), Observation of D^0 meson decays to $\pi^+\pi^-\mu^+\mu^-$ and $K^+K^-\mu^+\mu^-$ final states, Phys. Rev. Lett. **119**, 181805 (2017).
[11] R. Aaij *et al.* (LHCb Collaboration), Search for $D^+_{(s)} \to \pi^+\mu^+\mu^-$ and $D^+_{(s)} \to \pi^-\mu^+\mu^+$ decays, Phys. Lett. B **724**, 203 (2013).
[12] A. A. Alves, Jr. *et al.* (LHCb Collaboration), The LHCb detector at the LHC, J. Instrum. **3**, S08005 (2008).
[13] R. Aaij *et al.* (LHCb Collaboration), LHCb detector performance, Int. J. Mod. Phys. A **30**, 1530022 (2015).
[14] R. Aaij *et al.*, Performance of the LHCb Vertex Locator, J. Instrum. **9**, P09007 (2014).
[15] R. Arink *et al.*, Performance of the LHCb Outer Tracker, J. Instrum. **9**, P01002 (2014).
[16] M. Adinolfi *et al.*, Performance of the LHCb RICH detector at the LHC, Eur. Phys. J. C **73**, 2431 (2013).
[17] A. A. Alves, Jr. *et al.*, Performance of the LHCb muon system, J. Instrum. **8**, P02022 (2013).
[18] R. Aaij *et al.*, The LHCb trigger and its performance in 2011, J. Instrum. **8**, P04022 (2013).
[19] T. Sjöstrand, S. Mrenna, and P. Skands, PYTHIA 6.4 physics and manual, J. High Energy Phys. 05 (2006) 026; A brief introduction to PYTHIA 8.1, Comput. Phys. Commun. **178**, 852 (2008).
[20] I. Belyaev *et al.*, Handling of the generation of primary events in Gauss, the LHCb simulation framework, J. Phys. Conf. Ser. **331**, 032047 (2011).
[21] D. J. Lange, The EvtGen particle decay simulation package, Nucl. Instrum. Methods Phys. Res., Sect. A **462**, 152 (2001).
[22] P. Golonka and Z. Was, PHOTOS Monte Carlo: A precision tool for QED corrections in Z and W decays, Eur. Phys. J. C **45**, 97 (2006).
[23] J. Allison *et al.* (Geant4 Collaboration), Geant4 developments and applications, IEEE Trans. Nucl. Sci. **53**, 270 (2006); S. Agostinelli *et al.* (Geant4 Collaboration), Geant4: A simulation toolkit, Nucl. Instrum. Methods Phys. Res., Sect. A **506**, 250 (2003).
[24] M. Clemencic, G. Corti, S. Easo, C. R. Jones, S. Miglioranzi, M. Pappagallo, and P. Robbe, The LHCb simulation application, Gauss: Design, evolution and experience, J. Phys. Conf. Ser. **331**, 032023 (2011).
[25] R. Aaij *et al.* (LHCb Collaboration), Measurement of B meson production cross-sections in proton-proton collisions at $\sqrt{s} = 7$ TeV, J. High Energy Phys. 08 (2013) 117.

[26] R. Aaij *et al.* (LHCb Collaboration), Prompt charm production in pp collisions at $\sqrt{s} = 7$ TeV, Nucl. Phys. **B871**, 1 (2013).
[27] A. Blum, A. Kalai, and J. Langford, in *Proceedings of the Twelfth Annual Conference on Computational Learning Theory, COLT '99* (1999), p. 203.
[28] T. Skwarnicki, Ph.D. thesis, Institute of Nuclear Physics, Krakow, 1986, DESY-F31-86-02.
[29] A. L. Read, Presentation of search results: The CL_s technique, J. Phys. G **28**, 2693 (2002).
[30] S. S. Wilks, The large-sample distribution of the likelihood ratio for testing composite hypotheses, Ann. Math. Stat. **9**, 60 (1938).
[31] C. Patrignani *et al.* (Particle Data Group Collaboration), Review of particle physics, Chin. Phys. C **40**, 100001 (2016).

R. Aaij,[40] B. Adeva,[39] M. Adinolfi,[48] Z. Ajaltouni,[5] S. Akar,[59] J. Albrecht,[10] F. Alessio,[40] M. Alexander,[53] A. Alfonso Albero,[38] S. Ali,[43] G. Alkhazov,[31] P. Alvarez Cartelle,[55] A. A. Alves Jr.,[59] S. Amato,[2] S. Amerio,[23] Y. Amhis,[7] L. An,[3] L. Anderlini,[18] G. Andreassi,[41] M. Andreotti,[17,g] J. E. Andrews,[60] R. B. Appleby,[56] F. Archilli,[43] P. d'Argent,[12] J. Arnau Romeu,[6] A. Artamonov,[37] M. Artuso,[61] E. Aslanides,[6] M. Atzeni,[42] G. Auriemma,[26] M. Baalouch,[5] I. Babuschkin,[56] S. Bachmann,[12] J. J. Back,[50] A. Badalov,[38,m] C. Baesso,[62] S. Baker,[55] V. Balagura,[7,b] W. Baldini,[17] A. Baranov,[35] R. J. Barlow,[56] C. Barschel,[40] S. Barsuk,[7] W. Barter,[56] F. Baryshnikov,[32] V. Batozskaya,[29] V. Battista,[41] A. Bay,[41] L. Beaucourt,[4] J. Beddow,[53] F. Bedeschi,[24] I. Bediaga,[1] A. Beiter,[61] L. J. Bel,[43] N. Beliy,[63] V. Bellee,[41] N. Belloli,[21,i] K. Belous,[37] I. Belyaev,[32,40] E. Ben-Haim,[8] G. Bencivenni,[19] S. Benson,[43] S. Beranek,[9] A. Berezhnoy,[33] R. Bernet,[42] D. Berninghoff,[12] E. Bertholet,[8] A. Bertolin,[23] C. Betancourt,[42] F. Betti,[15] M. O. Bettler,[40] M. van Beuzekom,[43] Ia. Bezshyiko,[42] S. Bifani,[47] P. Billoir,[8] A. Birnkraut,[10] A. Bizzeti,[18,u] M. Bjørn,[57] T. Blake,[50] F. Blanc,[41] S. Blusk,[61] V. Bocci,[26] T. Boettcher,[58] A. Bondar,[36,w] N. Bondar,[31] I. Bordyuzhin,[32] S. Borghi,[56,40] M. Borisyak,[35] M. Borsato,[39] F. Bossu,[7] M. Boubdir,[9] T. J. V. Bowcock,[54] E. Bowen,[42] C. Bozzi,[17,40] S. Braun,[12] J. Brodzicka,[27] D. Brundu,[16] E. Buchanan,[48] C. Burr,[56] A. Bursche,[16,f] J. Buytaert,[40] W. Byczynski,[40] S. Cadeddu,[16] H. Cai,[64] R. Calabrese,[17,g] R. Calladine,[47] M. Calvi,[21,i] M. Calvo Gomez,[38,m] A. Camboni,[38,m] P. Campana,[19] D. H. Campora Perez,[40] L. Capriotti,[56] A. Carbone,[15,e] G. Carboni,[25,j] R. Cardinale,[20,h] A. Cardini,[16] P. Carniti,[21,i] L. Carson,[52] K. Carvalho Akiba,[2] G. Casse,[54] L. Cassina,[21] M. Cattaneo,[40] G. Cavallero,[20,40,h] R. Cenci,[24,t] D. Chamont,[7] M. G. Chapman,[48] M. Charles,[8] Ph. Charpentier,[40] G. Chatzikonstantinidis,[47] M. Chefdeville,[4] S. Chen,[16] S. F. Cheung,[57] S.-G. Chitic,[40] V. Chobanova,[39] M. Chrzaszcz,[42] A. Chubykin,[31] P. Ciambrone,[19] X. Cid Vidal,[39] G. Ciezarek,[40] P. E. L. Clarke,[52] M. Clemencic,[40] H. V. Cliff,[49] J. Closier,[40] V. Coco,[40] J. Cogan,[6] E. Cogneras,[5] V. Cogoni,[16,f] L. Cojocariu,[30] P. Collins,[40] T. Colombo,[40] A. Comerma-Montells,[12] A. Contu,[16] G. Coombs,[40] S. Coquereau,[38] G. Corti,[40] M. Corvo,[17,g] C. M. Costa Sobral,[50] B. Couturier,[40] G. A. Cowan,[52] D. C. Craik,[58] A. Crocombe,[50] M. Cruz Torres,[1] R. Currie,[52] C. D'Ambrosio,[40] F. Da Cunha Marinho,[2] C. L. Da Silva,[73] E. Dall'Occo,[43] J. Dalseno,[48] A. Davis,[3] O. De Aguiar Francisco,[40] K. De Bruyn,[40] S. De Capua,[56] M. De Cian,[12] J. M. De Miranda,[1] L. De Paula,[2] M. De Serio,[14,d] P. De Simone,[19] C. T. Dean,[53] D. Decamp,[4] L. Del Buono,[8] H.-P. Dembinski,[11] M. Demmer,[10] A. Dendek,[28] D. Derkach,[35] O. Deschamps,[5] F. Dettori,[54] B. Dey,[65] A. Di Canto,[40] P. Di Nezza,[19] H. Dijkstra,[40] F. Dordei,[40] M. Dorigo,[40] A. Dosil Suárez,[39] L. Douglas,[53] A. Dovbnya,[45] K. Dreimanis,[54] L. Dufour,[43] G. Dujany,[8] P. Durante,[40] J. M. Durham,[73] D. Dutta,[56] R. Dzhelyadin,[37] M. Dziewiecki,[12] A. Dziurda,[40] A. Dzyuba,[31] S. Easo,[51] U. Egede,[55] V. Egorychev,[32] S. Eidelman,[36,w] S. Eisenhardt,[52] U. Eitschberger,[10] R. Ekelhof,[10] L. Eklund,[53] S. Ely,[61] S. Esen,[12] H. M. Evans,[49] T. Evans,[57] A. Falabella,[15] N. Farley,[47] S. Farry,[54] D. Fazzini,[21,i] L. Federici,[25] D. Ferguson,[52] G. Fernandez,[38] P. Fernandez Declara,[40] A. Fernandez Prieto,[39] F. Ferrari,[15] L. Ferreira Lopes,[41] F. Ferreira Rodrigues,[2] M. Ferro-Luzzi,[40] S. Filippov,[34] R. A. Fini,[14] M. Fiorini,[17,g] M. Firlej,[28] C. Fitzpatrick,[41] T. Fiutowski,[28] F. Fleuret,[7,b] M. Fontana,[16,40] F. Fontanelli,[20,h] R. Forty,[40] V. Franco Lima,[54] M. Frank,[40] C. Frei,[40] J. Fu,[22,q] W. Funk,[40] E. Furfaro,[25,j] C. Färber,[40] E. Gabriel,[52] A. Gallas Torreira,[39] D. Galli,[15,e] S. Gallorini,[23] S. Gambetta,[52] M. Gandelman,[2] P. Gandini,[22] Y. Gao,[3] L. M. Garcia Martin,[71] J. García Pardiñas,[39] J. Garra Tico,[49] L. Garrido,[38] D. Gascon,[38] C. Gaspar,[40] L. Gavardi,[10] G. Gazzoni,[5] D. Gerick,[12] E. Gersabeck,[56] M. Gersabeck,[56] T. Gershon,[50] Ph. Ghez,[4] S. Gianì,[41] V. Gibson,[49] O. G. Girard,[41] L. Giubega,[30] K. Gizdov,[52] V. V. Gligorov,[8] D. Golubkov,[32] A. Golutvin,[55,69] A. Gomes,[1,a] I. V. Gorelov,[33] C. Gotti,[21,i] E. Govorkova,[43] J. P. Grabowski,[12] R. Graciani Diaz,[38] L. A. Granado Cardoso,[40] E. Graugés,[38] E. Graverini,[42] G. Graziani,[18] A. Grecu,[30] R. Greim,[9] P. Griffith,[16] L. Grillo,[56] L. Gruber,[40] B. R. Gruberg Cazon,[57] O. Grünberg,[67] E. Gushchin,[34] Yu. Guz,[37] T. Gys,[40] C. Göbel,[62] T. Hadavizadeh,[57] C. Hadjivasiliou,[5] G. Haefeli,[41] C. Haen,[40] S. C. Haines,[49] B. Hamilton,[60] X. Han,[12] T. H. Hancock,[57]

S. Hansmann-Menzemer,[12] N. Harnew,[57] S. T. Harnew,[48] C. Hasse,[40] M. Hatch,[40] J. He,[63] M. Hecker,[55] K. Heinicke,[10] A. Heister,[9] K. Hennessy,[54] P. Henrard,[5] L. Henry,[71] E. van Herwijnen,[40] M. Heß,[67] A. Hicheur,[2] D. Hill,[57] P. H. Hopchev,[41] W. Hu,[65] W. Huang,[63] Z. C. Huard,[59] W. Hulsbergen,[43] T. Humair,[55] M. Hushchyn,[35] D. Hutchcroft,[54] P. Ibis,[10] M. Idzik,[28] P. Ilten,[47] R. Jacobsson,[40] J. Jalocha,[57] E. Jans,[43] A. Jawahery,[60] M. Jezabek,[27] F. Jiang,[3] M. John,[57] D. Johnson,[40] C. R. Jones,[49] C. Joram,[40] B. Jost,[40] N. Jurik,[57] S. Kandybei,[45] M. Karacson,[40] J. M. Kariuki,[48] S. Karodia,[53] N. Kazeev,[35] M. Kecke,[12] F. Keizer,[49] M. Kelsey,[61] M. Kenzie,[49] T. Ketel,[44] E. Khairullin,[35] B. Khanji,[12] C. Khurewathanakul,[41] K. E. Kim,[61] T. Kirn,[9] S. Klaver,[19] K. Klimaszewski,[29] T. Klimkovich,[11] S. Koliiev,[46] M. Kolpin,[12] R. Kopecna,[12] P. Koppenburg,[43] A. Kosmyntseva,[32] S. Kotriakhova,[31] M. Kozeiha,[5] L. Kravchuk,[34] M. Kreps,[50] F. Kress,[55] P. Krokovny,[36,w] W. Krzemien,[29] W. Kucewicz,[27,l] M. Kucharczyk,[27] V. Kudryavtsev,[36,w] A. K. Kuonen,[41] T. Kvaratskheliya,[32,40] D. Lacarrere,[40] G. Lafferty,[56] A. Lai,[16] G. Lanfranchi,[19] C. Langenbruch,[9] T. Latham,[50] C. Lazzeroni,[47] R. Le Gac,[6] A. Leflat,[33,40] J. Lefrançois,[7] R. Lefèvre,[5] F. Lemaitre,[40] E. Lemos Cid,[39] O. Leroy,[6] T. Lesiak,[27] B. Leverington,[12] P.-R. Li,[63] T. Li,[3] Y. Li,[7] Z. Li,[61] X. Liang,[61] T. Likhomanenko,[68] R. Lindner,[40] F. Lionetto,[42] V. Lisovskyi,[7] X. Liu,[3] D. Loh,[50] A. Loi,[16] I. Longstaff,[53] J. H. Lopes,[2] D. Lucchesi,[23,o] M. Lucio Martinez,[39] H. Luo,[52] A. Lupato,[23] E. Luppi,[17,g] O. Lupton,[40] A. Lusiani,[24] X. Lyu,[63] F. Machefert,[7] F. Maciuc,[30] V. Macko,[41] P. Mackowiak,[10] S. Maddrell-Mander,[48] O. Maev,[31,40] K. Maguire,[56] D. Maisuzenko,[31] M. W. Majewski,[28] S. Malde,[57] B. Malecki,[27] A. Malinin,[68] T. Maltsev,[36,w] G. Manca,[16,f] G. Mancinelli,[6] D. Marangotto,[22,q] J. Maratas,[5,v] J. F. Marchand,[4] U. Marconi,[15] C. Marin Benito,[38] M. Marinangeli,[41] P. Marino,[41] J. Marks,[12] G. Martellotti,[26] M. Martin,[6] M. Martinelli,[41] D. Martinez Santos,[39] F. Martinez Vidal,[71] A. Massafferri,[1] R. Matev,[40] A. Mathad,[50] Z. Mathe,[40] C. Matteuzzi,[21] A. Mauri,[42] E. Maurice,[7,b] B. Maurin,[41] A. Mazurov,[47] M. McCann,[55,40] A. McNab,[56] R. McNulty,[13] J. V. Mead,[54] B. Meadows,[59] C. Meaux,[6] F. Meier,[10] N. Meinert,[67] D. Melnychuk,[29] M. Merk,[43] A. Merli,[22,40,q] E. Michielin,[23] D. A. Milanes,[66] E. Millard,[50] M.-N. Minard,[4] L. Minzoni,[17] D. S. Mitzel,[12] A. Mogini,[8] J. Molina Rodriguez,[1] T. Mombächer,[10] I. A. Monroy,[66] S. Monteil,[5] M. Morandin,[23] M. J. Morello,[24,t] O. Morgunova,[68] J. Moron,[28] A. B. Morris,[52] R. Mountain,[61] F. Muheim,[52] M. Mulder,[43] D. Müller,[40] J. Müller,[10] K. Müller,[42] V. Müller,[10] P. Naik,[48] T. Nakada,[41] R. Nandakumar,[51] A. Nandi,[57] I. Nasteva,[2] M. Needham,[52] N. Neri,[22,40] S. Neubert,[12] N. Neufeld,[40] M. Neuner,[12] T. D. Nguyen,[41] C. Nguyen-Mau,[41,n] S. Nieswand,[9] R. Niet,[10] N. Nikitin,[33] T. Nikodem,[12] A. Nogay,[68] D. P. O'Hanlon,[50] A. Oblakowska-Mucha,[28] V. Obraztsov,[37] S. Ogilvy,[19] R. Oldeman,[16,f] C. J. G. Onderwater,[72] A. Ossowska,[27] J. M. Otalora Goicochea,[2] P. Owen,[42] A. Oyanguren,[71] P. R. Pais,[41] A. Palano,[14] M. Palutan,[19,40] G. Panshin,[70] A. Papanestis,[51] M. Pappagallo,[52] L. L. Pappalardo,[17,g] W. Parker,[60] C. Parkes,[56] G. Passaleva,[18,40] A. Pastore,[14,d] M. Patel,[55] C. Patrignani,[15,e] A. Pearce,[40] A. Pellegrino,[43] G. Penso,[26] M. Pepe Altarelli,[40] S. Perazzini,[40] D. Pereima,[32] P. Perret,[5] L. Pescatore,[41] K. Petridis,[48] A. Petrolini,[20,h] A. Petrov,[68] M. Petruzzo,[22,q] E. Picatoste Olloqui,[38] B. Pietrzyk,[4] G. Pietrzyk,[41] M. Pikies,[27] D. Pinci,[26] F. Pisani,[40] A. Pistone,[20,h] A. Piucci,[12] V. Placinta,[30] S. Playfer,[52] M. Plo Casasus,[39] F. Polci,[8] M. Poli Lener,[19] A. Poluektov,[50] I. Polyakov,[61] E. Polycarpo,[2] G. J. Pomery,[48] S. Ponce,[40] A. Popov,[37] D. Popov,[11,40] S. Poslavskii,[37] C. Potterat,[2] E. Price,[48] J. Prisciandaro,[39] C. Prouve,[48] V. Pugatch,[46] A. Puig Navarro,[42] H. Pullen,[57] G. Punzi,[24,p] W. Qian,[50] J. Qin,[63] R. Quagliani,[8] B. Quintana,[5] B. Rachwal,[28] J. H. Rademacker,[48] M. Rama,[24] M. Ramos Pernas,[39] M. S. Rangel,[2] I. Raniuk,[45,†] F. Ratnikov,[35,x] G. Raven,[44] M. Ravonel Salzgeber,[40] M. Reboud,[4] F. Redi,[41] S. Reichert,[10] A. C. dos Reis,[1] C. Remon Alepuz,[71] V. Renaudin,[7] S. Ricciardi,[51] S. Richards,[48] M. Rihl,[40] K. Rinnert,[54] P. Robbe,[7] A. Robert,[8] A. B. Rodrigues,[41] E. Rodrigues,[59] J. A. Rodriguez Lopez,[66] A. Rogozhnikov,[35] S. Roiser,[40] A. Rollings,[57] V. Romanovskiy,[37] A. Romero Vidal,[39,40] M. Rotondo,[19] M. S. Rudolph,[61] T. Ruf,[40] P. Ruiz Valls,[71] J. Ruiz Vidal,[71] J. J. Saborido Silva,[39] E. Sadykhov,[32] N. Sagidova,[31] B. Saitta,[16,f] V. Salustino Guimaraes,[62] C. Sanchez Mayordomo,[71] B. Sanmartin Sedes,[39] R. Santacesaria,[26] C. Santamarina Rios,[39] M. Santimaria,[19] E. Santovetti,[25,j] G. Sarpis,[56] A. Sarti,[19,k] C. Satriano,[26,s] A. Satta,[25] D. M. Saunders,[48] D. Savrina,[32,33] S. Schael,[9] M. Schellenberg,[10] M. Schiller,[53] H. Schindler,[40] M. Schmelling,[11] T. Schmelzer,[10] B. Schmidt,[40] O. Schneider,[41] A. Schopper,[40] H. F. Schreiner,[59] M. Schubiger,[41] M. H. Schune,[7] R. Schwemmer,[40] B. Sciascia,[19] A. Sciubba,[26,k] A. Semennikov,[32] E. S. Sepulveda,[8] A. Sergi,[47] N. Serra,[42] J. Serrano,[6] L. Sestini,[23] P. Seyfert,[40] M. Shapkin,[37] Y. Shcheglov,[31] T. Shears,[54] L. Shekhtman,[36,w] V. Shevchenko,[68] B. G. Siddi,[17] R. Silva Coutinho,[42] L. Silva de Oliveira,[2] G. Simi,[23,o] S. Simone,[14,d] M. Sirendi,[49] N. Skidmore,[48] T. Skwarnicki,[61] I. T. Smith,[52] J. Smith,[49] M. Smith,[55] l. Soares Lavra,[1] M. D. Sokoloff,[59] F. J. P. Soler,[53] B. Souza De Paula,[2] B. Spaan,[10] P. Spradlin,[53] F. Stagni,[40] M. Stahl,[12] S. Stahl,[40] P. Stefko,[41] S. Stefkova,[55] O. Steinkamp,[42] S. Stemmle,[12] O. Stenyakin,[37] M. Stepanova,[31] H. Stevens,[10] S. Stone,[61] B. Storaci,[42] S. Stracka,[24,p] M. E. Stramaglia,[41] M. Straticiuc,[30] U. Straumann,[42]

S. Strokov,[70] J. Sun,[3] L. Sun,[64] K. Swientek,[28] V. Syropoulos,[44] T. Szumlak,[28] M. Szymanski,[63] S. T'Jampens,[4] A. Tayduganov,[6] T. Tekampe,[10] G. Tellarini,[17,g] F. Teubert,[40] E. Thomas,[40] J. van Tilburg,[43] M. J. Tilley,[55] V. Tisserand,[5] M. Tobin,[41] S. Tolk,[49] L. Tomassetti,[17,g] D. Tonelli,[24] R. Tourinho Jadallah Aoude,[1] E. Tournefier,[4] M. Traill,[53] M. T. Tran,[41] M. Tresch,[42] A. Trisovic,[49] A. Tsaregorodtsev,[6] P. Tsopelas,[43] A. Tully,[49] N. Tuning,[43,40] A. Ukleja,[29] A. Usachov,[7] A. Ustyuzhanin,[35] U. Uwer,[12] C. Vacca,[16,f] A. Vagner,[70] V. Vagnoni,[15,40] A. Valassi,[40] S. Valat,[40] G. Valenti,[15] R. Vazquez Gomez,[40] P. Vazquez Regueiro,[39] S. Vecchi,[17] M. van Veghel,[43] J. J. Velthuis,[48] M. Veltri,[18,r] G. Veneziano,[57] A. Venkateswaran,[61] T. A. Verlage,[9] M. Vernet,[5] M. Vesterinen,[57] J. V. Viana Barbosa,[40] D. Vieira,[63] M. Vieites Diaz,[39] H. Viemann,[67] X. Vilasis-Cardona,[38,m] M. Vitti,[49] V. Volkov,[33] A. Vollhardt,[42] B. Voneki,[40] A. Vorobyev,[31] V. Vorobyev,[36,w] C. Voß,[9] J. A. de Vries,[43] C. Vázquez Sierra,[43] R. Waldi,[67] J. Walsh,[24] J. Wang,[61] Y. Wang,[65] D. R. Ward,[49] H. M. Wark,[54] N. K. Watson,[47] D. Websdale,[55] A. Weiden,[42] C. Weisser,[58] M. Whitehead,[40] J. Wicht,[50] G. Wilkinson,[57] M. Wilkinson,[61] M. Williams,[56] M. Williams,[58] T. Williams,[47] F. F. Wilson,[51,40] J. Wimberley,[60] M. Winn,[7] J. Wishahi,[10] W. Wislicki,[29] M. Witek,[27] G. Wormser,[7] S. A. Wotton,[49] K. Wyllie,[40] Y. Xie,[65] M. Xu,[65] Q. Xu,[63] Z. Xu,[3] Z. Xu,[4] Z. Yang,[3] Z. Yang,[60] Y. Yao,[61] H. Yin,[65] J. Yu,[65] X. Yuan,[61] O. Yushchenko,[37] K. A. Zarebski,[47] M. Zavertyaev,[11,c] L. Zhang,[3] Y. Zhang,[7] A. Zhelezov,[12] Y. Zheng,[63] X. Zhu,[3] V. Zhukov,[9,33] J. B. Zonneveld,[52] and S. Zucchelli[15]

(LHCb Collaboration)

[1]*Centro Brasileiro de Pesquisas Físicas (CBPF), Rio de Janeiro, Brazil*
[2]*Universidade Federal do Rio de Janeiro (UFRJ), Rio de Janeiro, Brazil*
[3]*Center for High Energy Physics, Tsinghua University, Beijing, China*
[4]*Univ. Grenoble Alpes, Univ. Savoie Mont Blanc, CNRS, IN2P3-LAPP, Annecy, France*
[5]*Clermont Université, Université Blaise Pascal, CNRS/IN2P3, LPC, Clermont-Ferrand, France*
[6]*Aix Marseille Univ, CNRS/IN2P3, CPPM, Marseille, France*
[7]*LAL, Univ. Paris-Sud, CNRS/IN2P3, Université Paris-Saclay, Orsay, France*
[8]*LPNHE, Université Pierre et Marie Curie, Université Paris Diderot, CNRS/IN2P3, Paris, France*
[9]*I. Physikalisches Institut, RWTH Aachen University, Aachen, Germany*
[10]*Fakultät Physik, Technische Universität Dortmund, Dortmund, Germany*
[11]*Max-Planck-Institut für Kernphysik (MPIK), Heidelberg, Germany*
[12]*Physikalisches Institut, Ruprecht-Karls-Universität Heidelberg, Heidelberg, Germany*
[13]*School of Physics, University College Dublin, Dublin, Ireland*
[14]*Sezione INFN di Bari, Bari, Italy*
[15]*Sezione INFN di Bologna, Bologna, Italy*
[16]*Sezione INFN di Cagliari, Cagliari, Italy*
[17]*Universita e INFN, Ferrara, Ferrara, Italy*
[18]*Sezione INFN di Firenze, Firenze, Italy*
[19]*Laboratori Nazionali dell'INFN di Frascati, Frascati, Italy*
[20]*Sezione INFN di Genova, Genova, Italy*
[21]*Sezione INFN di Milano Bicocca, Milano, Italy*
[22]*Sezione di Milano, Milano, Italy*
[23]*Sezione INFN di Padova, Padova, Italy*
[24]*Sezione INFN di Pisa, Pisa, Italy*
[25]*Sezione INFN di Roma Tor Vergata, Roma, Italy*
[26]*Sezione INFN di Roma La Sapienza, Roma, Italy*
[27]*Henryk Niewodniczanski Institute of Nuclear Physics Polish Academy of Sciences, Kraków, Poland*
[28]*AGH - University of Science and Technology, Faculty of Physics and Applied Computer Science, Kraków, Poland*
[29]*National Center for Nuclear Research (NCBJ), Warsaw, Poland*
[30]*Horia Hulubei National Institute of Physics and Nuclear Engineering, Bucharest-Magurele, Romania*
[31]*Petersburg Nuclear Physics Institute (PNPI), Gatchina, Russia*
[32]*Institute of Theoretical and Experimental Physics (ITEP), Moscow, Russia*
[33]*Institute of Nuclear Physics, Moscow State University (SINP MSU), Moscow, Russia*
[34]*Institute for Nuclear Research of the Russian Academy of Sciences (INR RAS), Moscow, Russia*
[35]*Yandex School of Data Analysis, Moscow, Russia*
[36]*Budker Institute of Nuclear Physics (SB RAS), Novosibirsk, Russia*
[37]*Institute for High Energy Physics (IHEP), Protvino, Russia*
[38]*ICCUB, Universitat de Barcelona, Barcelona, Spain*

[39]Instituto Galego de Física de Altas Enerxías (IGFAE), Universidade de Santiago de Compostela, Santiago de Compostela, Spain
[40]European Organization for Nuclear Research (CERN), Geneva, Switzerland
[41]Institute of Physics, Ecole Polytechnique Fédérale de Lausanne (EPFL), Lausanne, Switzerland
[42]Physik-Institut, Universität Zürich, Zürich, Switzerland
[43]Nikhef National Institute for Subatomic Physics, Amsterdam, The Netherlands
[44]Nikhef National Institute for Subatomic Physics and VU University Amsterdam, Amsterdam, The Netherlands
[45]NSC Kharkiv Institute of Physics and Technology (NSC KIPT), Kharkiv, Ukraine
[46]Institute for Nuclear Research of the National Academy of Sciences (KINR), Kyiv, Ukraine
[47]University of Birmingham, Birmingham, United Kingdom
[48]H.H. Wills Physics Laboratory, University of Bristol, Bristol, United Kingdom
[49]Cavendish Laboratory, University of Cambridge, Cambridge, United Kingdom
[50]Department of Physics, University of Warwick, Coventry, United Kingdom
[51]STFC Rutherford Appleton Laboratory, Didcot, United Kingdom
[52]School of Physics and Astronomy, University of Edinburgh, Edinburgh, United Kingdom
[53]School of Physics and Astronomy, University of Glasgow, Glasgow, United Kingdom
[54]Oliver Lodge Laboratory, University of Liverpool, Liverpool, United Kingdom
[55]Imperial College London, London, United Kingdom
[56]School of Physics and Astronomy, University of Manchester, Manchester, United Kingdom
[57]Department of Physics, University of Oxford, Oxford, United Kingdom
[58]Massachusetts Institute of Technology, Cambridge, Massachusetts, USA
[59]University of Cincinnati, Cincinnati, Ohio, USA
[60]University of Maryland, College Park, Maryland, USA
[61]Syracuse University, Syracuse, New York, USA
[62]Pontifícia Universidade Católica do Rio de Janeiro (PUC-Rio), Rio de Janeiro, Brazil, associated to Universidade Federal do Rio de Janeiro (UFRJ), Rio de Janeiro, Brazil
[63]University of Chinese Academy of Sciences, Beijing, China, associated to Center for High Energy Physics, Tsinghua University, Beijing, China
[64]School of Physics and Technology, Wuhan University, Wuhan, China, associated to Center for High Energy Physics, Tsinghua University, Beijing, China
[65]Institute of Particle Physics, Central China Normal University, Wuhan, Hubei, China, associated to Center for High Energy Physics, Tsinghua University, Beijing, China
[66]Departamento de Fisica, Universidad Nacional de Colombia, Bogota, Colombia, associated to LPNHE, Université Pierre et Marie Curie, Université Paris Diderot, CNRS/IN2P3, Paris, France
[67]Institut für Physik, Universität Rostock, Rostock, Germany, associated to Physikalisches Institut, Ruprecht-Karls-Universität Heidelberg, Heidelberg, Germany
[68]National Research Centre Kurchatov Institute, Moscow, Russia, associated to Institute of Theoretical and Experimental Physics (ITEP), Moscow, Russia
[69]National University of Science and Technology MISIS, Moscow, Russia, associated to Institute of Theoretical and Experimental Physics (ITEP), Moscow, Russia
[70]National Research Tomsk Polytechnic University, Tomsk, Russia, associated to Institute of Theoretical and Experimental Physics (ITEP), Moscow, Russia
[71]Instituto de Fisica Corpuscular, Centro Mixto Universidad de Valencia - CSIC, Valencia, Spain, associated to ICCUB, Universitat de Barcelona, Barcelona, Spain
[72]Van Swinderen Institute, University of Groningen, Groningen, The Netherlands, associated to Nikhef National Institute for Subatomic Physics, Amsterdam, The Netherlands
[73]Los Alamos National Laboratory (LANL), Los Alamos, United States, associated to Syracuse University, Syracuse, New York, USA

†Deceased.
[a]Aslo at Universidade Federal do Triângulo Mineiro (UFTM), Uberaba-MG, Brazil.
[b]Aslo at Laboratoire Leprince-Ringuet, Palaiseau, France.
[c]Aslo at P.N. Lebedev Physical Institute, Russian Academy of Science (LPI RAS), Moscow, Russia.
[d]Aslo at Università di Bari, Bari, Italy.
[e]Aslo at Università di Bologna, Bologna, Italy.
[f]Aslo at Università di Cagliari, Cagliari, Italy.
[g]Aslo at Università di Ferrara, Ferrara, Italy.
[h]Aslo at Università di Genova, Genova, Italy.
[i]Aslo at Università di Milano Bicocca, Milano, Italy.

[j]Aslo at Università di Roma Tor Vergata, Roma, Italy.
[k]Aslo at Università di Roma La Sapienza, Roma, Italy.
[l]Aslo at AGH - University of Science and Technology, Faculty of Computer Science, Electronics and Telecommunications, Kraków, Poland.
[m]Aslo at LIFAELS, La Salle, Universitat Ramon Llull, Barcelona, Spain.
[n]Aslo at Hanoi University of Science, Hanoi, Vietnam.
[o]Aslo at Università di Padova, Padova, Italy.
[p]Aslo at Università di Pisa, Pisa, Italy.
[q]Aslo at Università degli Studi di Milano, Milano, Italy.
[r]Aslo at Università di Urbino, Urbino, Italy.
[s]Aslo at Università della Basilicata, Potenza, Italy.
[t]Aslo at Scuola Normale Superiore, Pisa, Italy.
[u]Aslo at Università di Modena e Reggio Emilia, Modena, Italy.
[v]Aslo at Iligan Institute of Technology (IIT), Iligan, Philippines.
[w]Aslo at Novosibirsk State University, Novosibirsk, Russia.
[x]Aslo at National Research University Higher School of Economics, Moscow, Russia.